Controllable interaction of counterpropagating solitons in three-level media

Andreas Pusch,* Joachim M. Hamm, and Ortwin Hess†
Advanced Technology Institute and Department of Physics, Faculty of Engineering and Physical Sciences, University of Surrey, Guildford, GU2 7XH, United Kingdom
(Received 16 June 2010; published 11 August 2010)

We examine the dynamics of counterpropagating self-induced transparency solitons in three-level media. In a multilevel system, self-induced transparency gives rise to soliton solutions if the propagation is unidirectional, but the collision of counterpropagating pulses destroys the integrability of the underlying equations. We consider the collision of a rightward and a leftward moving self-induced transparency solitary wave by solving the full Maxwell-Bloch equations numerically using a finite-difference time-domain approach. Depending on pulse duration, amplitude and relative polarizations of the initial solitary waves we observe different regimes of interaction. For high group velocities and orthogonal polarizations, secondary solitary waves are born during the interaction, whereas the collision of solitary waves with the same polarization never produces secondary solitary waves but leaves behind a population grating in the interaction region. Because the crucial parameters can be controlled, an experimental confirmation of the predicted interaction regimes should be feasible.

DOI: 10.1103/PhysRevA.82.023805 PACS number(s): 42.65.Tg, 42.50.Md

I. INTRODUCTION

Since their discovery by John Scott Russell in water waves in 1834 [1] solitons have attracted interest from various areas of research, especially in the field of nonlinear optics. Solitons have been found to exist in various optical media, with Kerr [2], Raman [3] or quadratic nonlinearities [4], in photorefractive materials [5], and in two-level self-induced transparency media [6]. Contrary to solitons in the strict mathematical sense, which retain their shape when penetrating each other, these particlelike solutions are prone to change upon mutual interaction. In a collision process they can dissipate or exchange energy, merge, annihilate each other, or give birth to additional solitary waves. Theoretical studies have been conducted on collisions of solitons in two- and three-level media [7–9], in birefringent optical fibers [10,11], and interactions of optical spatial solitons [12,13]. Experiments on soliton collisions in photorefractive materials [14] have been performed confirming the possibility of the annihilation of solitons [15], and the merging or birth of solitons [16,17]. Recently, the creation of dispersive waves has been observed in the collision of solitons in a photonic crystal fiber [18].

Self-induced transparency (SIT) solitons were the first solitons discovered in optical systems by McCall and Hahn in 1967 [6,19]. These nonlinear solutions retain amplitude and shape upon propagation through an absorbing two-level medium by inducing a complete rotation of the Bloch vector of the two-level system as the gain via stimulated emission into the trailing edge equals the absorption loss of the leading edge. Because of this complete rotation of the Bloch vector the fundamental SIT solitons are usually referred to as 2π pulses.

Further analytical studies of SIT solitons have relaxed some of the assumptions on the temporal and spatial dependencies of the electric field, which were initially made by McCall and Hahn to obtain the SIT equations [19]. The reduced Maxwell-Bloch (RMB) equations, unidirectional propagation equations which neither make use of the slowly varying envelope approximation (SVEA) nor the rotating wave approximation (RWA), are still integrable [20,21]. Notably, the two-soliton (breather) solution of the RMB equations is a generalization of the 2π pulse solution of the SIT equations in SVEA. When the assumption of the unidirectionality of the pulse propagation is lifted, the resulting equations are not integrable anymore and no soliton solution exists. A momentary violation of approximative unidirectional propagation (during the collision of counterpropagating pulses) can therefore lead to a whole spectrum of new effects such as breakup, birth, or annihilation of otherwise stable solitary waves.

Here, we systematically investigate the collision of counterpropagating simultons [22], SIT solitary waves in three-level media (Fig. 1), using an auxiliary differential equation finite-difference time-domain (ADE-FDTD) approach. This model introduces, apart from the numerical discretization, no approximations on either the directionality or the form of the electromagnetic field. Simultons have been found to be similar to SIT solitons in two-level systems [23–25], but offer an additional degree of freedom due to the possibility of distributing the excitation between two transitions. In this work we show that, in contrast to collisions in two-level media, collisions in three-level media allow for the birth of new (secondary) solitary waves. Furthermore, we demonstrate that the outcome of the collision in terms of the group velocities of the resulting pulses depends solely on the polarizations and group velocities of the initial pulses. For a practical realization the duration of the pulses should be considerably smaller than all relaxation times in the medium and an effectively one-dimensional system, such as a fiber, must be chosen.

The outline of the paper is as follows: In Sec. II we present the fundamental equations for the optical dipole interaction of a light pulse with a three-level medium in the full Maxwell-Bloch theory. The results of finite-difference time-domain (FDTD) simulations of the collision of counterpropagating simultons in a V-type three-level system are reported and

*a.pusch@surrey.ac.uk
†o.hess@surrey.ac.uk

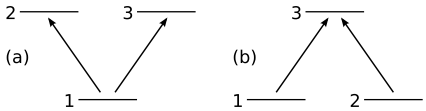

FIG. 1. Schematics of a V-type (a) and Λ-type (b) degenerate three-level medium.

discussed in Sec. III. We first study the collision of counterpropagating simultons with parallel relative polarization and show that this scenario is equivalent to the collision of simultons in two-level media (Sec. III A). Next, the collision of simultons with orthogonal polarizations is investigated in Sec. III B and finally we look at the collisions of simultons with arbitrary relative polarizations (Sec. III C). We conclude our findings in Sec. IV.

II. THREE-LEVEL MAXWELL-BLOCH EQUATIONS

We model the propagation of the light pulses using the FDTD method [26] for Maxwell's equations combined with Mur boundary conditions [27].

In a one-dimensional propagation scheme the relevant equations are the one-dimensional Maxwell equations for the electric and magnetic field with the macroscopic polarization, resulting from the material equations for the three-level medium, as source term. The state of the three-level medium at a given point in space x is represented by a three-by-three density matrix $\hat{\rho}(x,t)$ and its time evolution can be described by a three-by-three Hamiltonian $\hat{H}$ via the Liouville equation,

$$i\hbar\frac{\partial}{\partial t}\hat{\rho} = [\hat{\rho},\hat{H}]. \tag{1}$$

For a three-level system in dipole approximation the Hamiltonian can be written as

$$\hat{H} = \hat{H}_0 - \hat{\boldsymbol{\mu}}\cdot\mathbf{E} = \begin{bmatrix} \hbar\omega_1 & -\boldsymbol{\mu}_{12}\cdot\mathbf{E} & -\boldsymbol{\mu}_{13}\cdot\mathbf{E} \\ -\boldsymbol{\mu}_{12}^*\cdot\mathbf{E} & \hbar\omega_2 & -\boldsymbol{\mu}_{23}\cdot\mathbf{E} \\ -\boldsymbol{\mu}_{13}^*\cdot\mathbf{E} & -\boldsymbol{\mu}_{23}^*\cdot\mathbf{E} & \hbar\omega_3 \end{bmatrix}, \tag{2}$$

with $\mathbf{E} = E_x\mathbf{e}_x + E_y\mathbf{e}_y + E_z\mathbf{e}_z$ denoting the electrical field vector, $\boldsymbol{\mu}_{12} = \mu\mathbf{e}_y + i\mu\mathbf{e}_z$, $\boldsymbol{\mu}_{13} = \mu\mathbf{e}_y - i\mu\mathbf{e}_z$, and $\boldsymbol{\mu}_{23} = 0$ the vectors of dipole matrix elements, and $\hbar\omega_i$ the energy of level $|i\rangle$.

The Liouville equation (1) together with the Hamiltonian (2) results in the Bloch equations, equations of motion of the density matrix elements of a three-level system excited by a light field:

$$\frac{\partial}{\partial t}\rho_{12} = i[\rho_{12}(\omega_1-\omega_2) + \Omega_{12}(\rho_{11}-\rho_{22}) - \Omega_{13}\rho_{23}^*], \tag{3}$$

$$\frac{\partial}{\partial t}\rho_{13} = i[\rho_{13}(\omega_1-\omega_3) + \Omega_{13}(\rho_{11}-\rho_{33}) - \Omega_{12}\rho_{23}], \tag{4}$$

$$\frac{\partial}{\partial t}\rho_{23} = i[\rho_{23}(\omega_2-\omega_3) + \Omega_{13}\rho_{12}^* - \Omega_{12}^*\rho_{13}], \tag{5}$$

$$\frac{\partial}{\partial t}\rho_{11} = -2\,\mathrm{Im}\,(\Omega_{12}^*\rho_{12}) - 2\,\mathrm{Im}\,(\Omega_{13}^*\rho_{13}), \tag{6}$$

$$\frac{\partial}{\partial t}\rho_{22} = 2\,\mathrm{Im}\,(\Omega_{12}^*\rho_{12}). \tag{7}$$

$$\frac{\partial}{\partial t}\rho_{33} = 2\,\mathrm{Im}\,(\Omega_{13}^*\rho_{13}). \tag{8}$$

Here, $\Omega_{ij} = \boldsymbol{\mu}_{ij}\cdot\mathbf{E}_{\mathrm{loc}}/\hbar$ is the Rabi frequency for transition $|i\rangle \leftrightarrow |j\rangle$.

The macroscopic polarization density $\mathbf{P}$ is obtained as the sum of the real parts of the dipole matrix vectors multiplied by the coherences ρ_{ij},

$$\mathbf{P}(t) = n\,\mathrm{tr}\,[\hat{\rho}(t)\hat{\boldsymbol{\mu}}] = 2n\sum_{i\neq j}\mathrm{Re}\,[\boldsymbol{\mu}_{ij}^*\rho_{ij}(t)]. \tag{9}$$

Furthermore, we note that in a dense medium there is a difference between the macroscopic electric field used in the Maxwell equations and the microscopic field experienced by an atom in a certain local neighborhood. This difference is due to the polarization of the surrounding atoms which interacts with the atom. The local field acting on the atom is approximately given by [28]

$$\mathbf{E}_{\mathrm{loc}} = \mathbf{E} + \frac{\mathbf{P}}{3}. \tag{10}$$

The model equations are not integrable, due to their bidirectional nature and the addition of the local field correction (10). However, an undisturbed pulse with an area of 2π still propagates largely unchanged through the system as the local field correction only becomes important at significantly larger densities than used in this study [29]. Here, correction (10) is included to provide a more accurate description yet has been verified to not change the qualitative nature of our findings.

We use the total-field scattered-field method [30] to inject rightward (leftward) moving (secant hyperbolic-shaped) pulses into vacuum sections on the left (right) of the three-level medium. Reflections at the vacuum-medium boundaries are negligibly small for the parameters used.

III. COLLISION OF SIMULTONS IN A V-TYPE THREE-LEVEL MEDIUM

A. Collision of simultons with parallel polarizations

In this section we investigate the collision of two counterpropagating simultons with parallel polarizations in a V-type three-level medium. We assume that the dephasing times and the lifetimes of the upper states are much longer than the pulse duration and can therefore be neglected. In the case where both pulses have the same electromagnetic field polarization, one can reduce the three-level system to a two-level system by an appropriate choice of basis states. For example, if the simultons are y polarized, only the states $|1\rangle$ and $\frac{1}{\sqrt{2}}(|2\rangle + |3\rangle)$ can be occupied and constitute the two-level system of interest. Therefore, individual simultons in a three-level medium have the same shape as SIT solitons in two-level media even though they may interact with both transitions of the original quantum system. For a two-level medium, characterized by the vector of the dipole matrix elements $\boldsymbol{\mu}$, the resonance frequency ω and the particle density n, the temporal shape of 2π pulses (in SVEA) is well known [19] and follows the form,

$$\mathbf{E}(t) = \mathbf{E}_0\frac{\sin[\omega(t-t_0)]}{\cosh\left(1.76\frac{t-t_0}{\tau}\right)} = \frac{\mathbf{E}_0}{|\mathbf{E}_0|}\frac{\hbar}{\mu\tau}\frac{\sin[\omega(t-t_0)]}{\cosh\left(1.76\frac{t-t_0}{\tau}\right)}, \tag{11}$$

where τ is the pulse duration of the resonant pulse.

The group velocities of the 2π pulses are given by the following relation [19]:

$$v = \frac{c}{1 + \frac{2n\hbar\omega}{\epsilon_0 |\mathbf{E}_0|^2}} = \frac{c}{1 + \frac{2n\omega\mu^2\tau^2}{\epsilon_0\hbar}}. \tag{12}$$

These equations provide surprisingly good approximations for isolated solitary waves of the full Maxwell-Bloch equations down to pulse durations of a few optical cycles [31]. A solitary wave of pulse area 2π in a given two-level medium can therefore be fully characterized either by its group velocity, its duration, or the ratio of the electromagnetic energy to the energy deposited in the medium. We can thus choose the group velocity of the solitary wave in any given medium by setting appropriate values for the pulse duration τ.

Depending on the group velocities of the counterpropagating pulses, a collision either leads to a reduction in the pulse amplitude and group velocity, and a long-lived density excitation in the collision region, or to a complete breakup of the pulses. The relative orientation of the simulton polarization to the polarization of the three-level system has, however, no influence on the outcome of the collision. For high group velocities a reduction in the amplitude of the simulton occurs while some of its energy is transferred to an excitation of the medium and some is radiated off. Figure 2(a) shows the result of a collision where the simulton polarizations are chosen to interact with only one of the transitions in the three-level system, whereas Fig. 2(b) shows the outcome for linearly polarized simultons which are both interacting equally with both transitions of the three-level system. The dynamics of the field envelope is identical in these two scenarios because in both situations the three-level system can be reduced to a two-level system. The simultons lose energy during the inelastic collision, which results in a reduction of their group velocity and leaves a population grating in the interaction region. There is a difference in the population densities ρ_{22} and ρ_{33} between the circularly polarized and linearly polarized colliding pulses because we have not chosen the natural basis for the case of linear polarization.

For low group velocities the simultons break up into several breathers, solutions of the nonlinear equations with zero pulse area, (again) leaving a population grating in the interaction region [see Fig. 2(c)]. The critical group velocity below which the pulses break up is approximately given by $v_0 = 0.36c$. The dependence of the group velocity of the simultons after collision on the group velocity of the simultons before collision is shown in Fig. 3. The critical velocity is the velocity at which the velocity of the simulton after collision is zero (i.e., there is no simulton anymore). For high group velocities the velocity reduction during the collision is relatively small and it increases toward lower group velocities.

B. Collision of simultons with orthogonal polarizations

After having analyzed collisions of simultons with the same field polarization we focus now on the collision of simultons with orthogonal field polarizations, again in V-type media. As we will show, the birth of secondary simultons is possible in such a collision scheme. In Λ-type media with equal initial occupation probability of the lower states, such a result can also be obtained. As before, we assume that the dephasing times

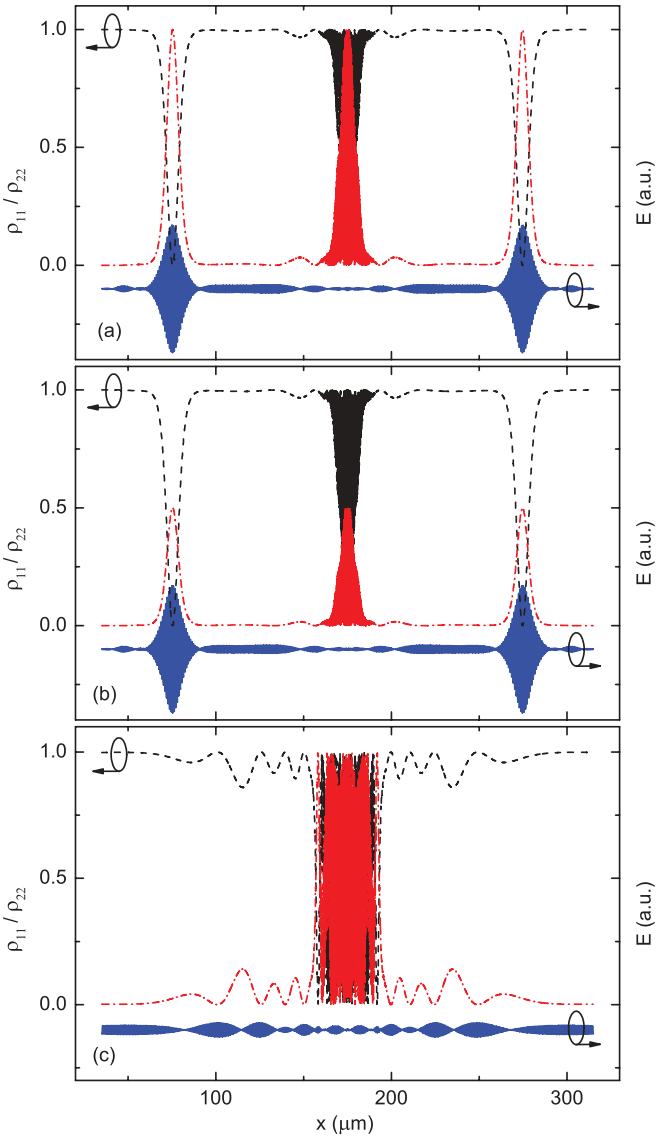

FIG. 2. (Color online) ρ_{11} (black dashed line), ρ_{22} (red dash-dotted line), and E (blue solid line) after the collision of two counterpropagating simultons against distance x for group velocities (a) $v_0 = 0.75c$, circularly polarized; (b) $v_0 = 0.75c$, linearly polarized; and (c) $v_0 = 0.35c$, circularly polarized. The material parameters are $\mu = 1.19 \times 10^{-29}$ C m, $n = 8.64 \times 10^{24}$ m^{-3}, and $\omega = 3.59 \times 10^{15}$ s^{-1}.

and the upper state lifetimes are much longer than the pulse durations, so that they can be neglected in the quantitative analysis. We find that the introduction of small dephasing rates into the Bloch equations [Eqs. (3)–(8)] does not have a significant impact on the results.

There are two distinct regimes in the collision of orthogonally polarized simultons. For initial group velocities lower than $v_0 \approx 0.62c$, the collision breaks the original simultons into at least two copropagating pulses which resemble the two-soliton solutions of the SIT equations in SVEA discussed by Steudel in [32]. These pulses are unable to invert the medium completely but propagate with a similar group velocity as 2π pulses of the same amplitude. An example of the pulse breakup is given in Fig. 4(a), where we plot the occupation probability

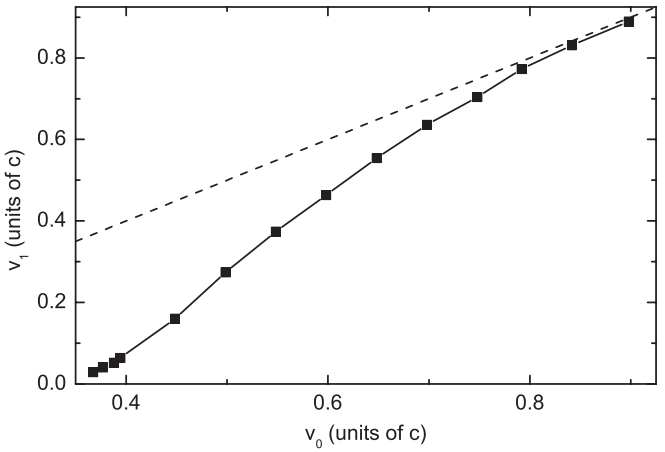

FIG. 3. Group velocity v_0 before collision versus group velocity v_1 after collision. The dashed line ($v_1 = v_0$) serves as a guide to the eye. Medium parameters are chosen as in Fig. 2.

ρ_{11} of the ground state of the three-level medium versus time and propagation distance for two counterpropagating simultons with an initial group velocity of $v_0 = 0.4c$. This contrasts with the observations in the case of parallel polarized simultons, where down to group velocities of $v_0 = 0.36c$ the initial simultons get reshaped to simultons of lower amplitude and group velocity. Furthermore, no population grating is left in the interaction region.

For initial group velocities higher than $v_0 \approx 0.62c$ a new phenomenon is observed: the birth of secondary solitary waves. During collision each of the original simultons breaks up into two simultons with different group velocities, thereby the energy of the initial simultons is distributed between the two resulting simultons. Additionally, some energy is dissipated in the interaction process. As the energy of a simulton of area 2π is inversely proportional to its duration and as a longer duration leads to a lower group velocity, the resulting simultons are slower than the initial simultons. Figures 4(c) and 4(d) show examples of the birth of secondary simultons for group velocities of $v_0 = 0.64c$ and $v_0 = 0.8c$, respectively. The secondary simultons still achieve maximum inversion ($\rho_{11} = 0$). It can be seen that the difference in group velocities between the resulting simultons is larger for the higher group velocity. If we denote the group velocity of the initial simultons as v_0, the group velocity of the remaining simulton as v_1 and the group velocity of the secondary simulton as v_2, then v_1 decreases and v_2 increases when v_0 decreases. For $v_0 = 0.62c$, v_2 has reached almost the same value as v_1. In this case, the two pulses initially exchange energy until they separate very slowly [see Fig. 4(b)]. The reason that no new simultons are created for initial group velocities $v_0 < 0.62c$ is that v_2 would have the same value as v_1.

We systematically investigated the dependencies of the group velocities v_1 and v_2 of the pulses created in the collision on the initial group velocity of the counterpropagating pulses and the parameters of the medium. The results are shown in Fig. 5. A first observation is that the velocities v_2 and v_1 do not depend on the parameters of the medium, which we varied broadly. This indicates that our results are still valid for picosecond pulses in a medium of much lower density, as

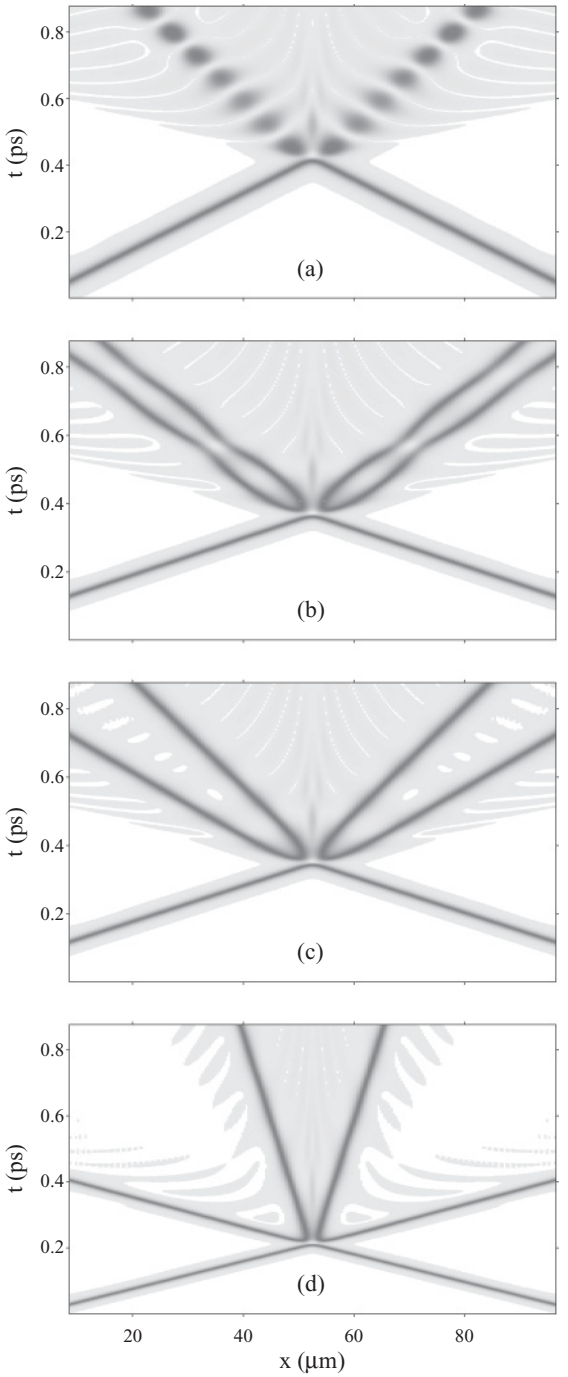

FIG. 4. Linear grayscale plot of the occupancy of the lowest level ρ_{11} during the collision of circularly polarized pulses with group velocities of (a) $v_0 = 0.4c$, (b) $v_0 = 0.62c$, (c) $v_0 = 0.64c$, and (d) $v_0 = 0.8c$. Black corresponds to $\rho_{11} = 0$ and white to $\rho_{11} = 1$. The material parameters are $\mu = 2.38 \times 10^{-29}\,\mathrm{C\,m}$, $\rho = 8.64 \times 10^{24}\,\mathrm{m^{-3}}$, and $\omega = 3.59 \times 10^{15}\,\mathrm{s^{-1}}$.

long as the dephasing times and spontaneous emission times are much longer than the pulse duration. Just as for the case of parallel polarized simultons, the dependence on group velocity is the only significant dependence for the case of orthogonal polarized pulses.

In Fig. 5 the measured group velocities v_1 and v_2 do show deviations to both sides of the fit. This could be a consequence

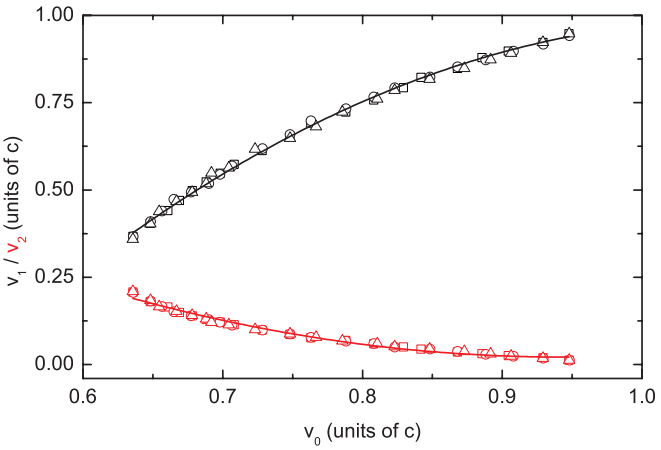

FIG. 5. (Color online) Group velocities of v_1 of primary pulses and v_2 of secondary pulses after collision plotted versus the group velocity of the initial pulses. Different symbols stand for different values of dipole moment μ and medium density n and the lines represent polynomial fits of second order to the data.

of a discretization of the possible group velocities [33] or due to slight errors introduced by the method of extracting the group velocities from the simulations. Extracting the group velocities involves comparing the positions of the maxima of the electric field envelopes at different times, but we only have the positions of the maximum electric field values available and those do not necessarily coincide exactly with the position of the maximum of the electric field envelope.

The velocities v_2 (Fig. 5) increase superlinearly when we approach the critical group velocity $v_0 = 0.62c$. The lower the group velocity, the higher the proportion of pulse energy which is split off into the secondary pulse. This is reflected in the dependence of v_1 on v_0. v_1 rises superlinearly with increasing initial group velocity v_0 and it approaches v_0 as v_0 approaches the speed of light.

In order to understand why collisions of orthogonal polarized simultons are fundamentally different from the collisions of simultons with the same polarization we analyze how this difference is reflected in the model equations. The coherence ρ_{23} between the two upper states plays a crucial role in the interaction between the colliding pulses, as it constitutes the main difference between a genuine three-level system (orthogonal polarizations) and an effective two-level system (parallel polarizations). Additionally, in the case of orthogonal polarizations, the pulses compete for the same population of the lower state without acting on the same transition. One pulse, therefore, impinges on a population gradient created by the other pulse and the pulses excite the coherence ρ_{23} between the two upper states when they collide. ρ_{23} is only excited in regions where both pulses are present and it acts back on the coherences ρ_{12} and ρ_{13} which constitute the optical polarization.

To establish the difference between the nonintegrable full Maxwell-Bloch equations in the case of counterpropagating solitons and the integrable reduced Maxwell-Bloch equations we analyze the case of a forward-moving electric field $E_y^+(x,t)$ and a backward-moving electric field $E_z^-(x,t)$. Both are resonant with the transition frequency of a degenerate V-type three-level system with dipole matrix elements $\boldsymbol{\mu}_{12} = \mu \mathbf{e_y}$ and $\boldsymbol{\mu}_{13} = \mu \mathbf{e_z}$. The wave equations for E_y^+ and E_z^- can be written in terms of the density matrix elements as

$$\frac{\partial^2 E_y^+}{\partial x^2} - \frac{1}{c^2}\frac{\partial^2 E_y^+}{\partial t^2} = \frac{2n\mu}{\epsilon_0 c^2}\frac{\partial^2 \mathrm{Re}\,(\rho_{12}^+)}{\partial t^2}, \tag{13}$$

$$\frac{\partial^2 E_z^-}{\partial x^2} - \frac{1}{c^2}\frac{\partial^2 E_z^-}{\partial t^2} = \frac{2n\mu}{\epsilon_0 c^2}\frac{\partial^2 \mathrm{Re}\,(\rho_{13}^-)}{\partial t^2}. \tag{14}$$

Let us analyze the left-hand side of Eq. (13) to see which terms will be added due to the interaction of counterpropagating pulses. We start with replacing the derivatives on the right-hand side by inserting Eqs. (3) and (5):

$$\begin{aligned}\frac{\partial^2 \mathrm{Re}\,(\rho_{12}^+)}{\partial t^2} &= \frac{\partial}{\partial t}[\,\mathrm{Im}\,(\rho_{12}^+)\omega - \Omega_z^-\,\mathrm{Im}\,(\rho_{23})] \\ &= -[\omega^2 + (\Omega_z^-)^2]\mathrm{Re}\,(\rho_{12}^+) + \omega\Omega_y^+(\rho_{11} - \rho_{22}) \\ &\quad - \omega\Omega_z^-\mathrm{Re}\,(\rho_{23}) - \frac{\partial \Omega_z^-}{\partial t}\,\mathrm{Im}\,(\rho_{23}) \\ &\quad + \Omega_z^-\Omega_y^+\mathrm{Re}\,(\rho_{13}^-).\end{aligned} \tag{15}$$

Replacing the densities ρ_{11} and ρ_{22} and the coherence term ρ_{23} with their integral form we can identify the terms which are due to the interaction of two counterpropagating pulses and those which are present in the case of a single pulse tuned to only one transition. The latter terms are the ones giving rise to self-induced transparency and the former are the ones responsible for the pulse breakup:

$$\begin{aligned}\rho_{11}(x,t) = 1 &- \int_0^t 2\Omega_y^+(x,t')\,\mathrm{Im}\,[\rho_{12}^+(x,t')]\,dt' \\ &- \int_0^t 2\Omega_z^-(x,t')\,\mathrm{Im}\,[\rho_{13}^-(x,t')]\,dt',\end{aligned} \tag{16}$$

$$\rho_{22}(x,t) = \int_0^t 2\Omega_y^+(x,t')\,\mathrm{Im}\,[\rho_{12}^+(x,t')]\,dt', \tag{17}$$

$$\begin{aligned}\mathrm{Re}\,[\rho_{23}(x,t)] = \int_0^t \{&\Omega_z^-(x,t')\,\mathrm{Im}\,[\rho_{12}^+(x,t')] \\ &+ \Omega_y^+(x,t')\,\mathrm{Im}\,[\rho_{13}^-(x,t')]\}\,dt'\end{aligned} \tag{18}$$

$$\begin{aligned}\mathrm{Im}\,[\rho_{23}(x,t)] = \int_0^t \{&\Omega_z^-(x,t')\,\mathrm{Re}\,[\rho_{12}^+(x,t')] \\ &- \Omega_y^+(x,t')\,\mathrm{Re}\,[\rho_{13}^-(x,t')]\}\,dt'.\end{aligned} \tag{19}$$

The last term in ρ_{11} is an interaction term which would also be present in the interaction of two colliding solitary waves in a two-level system. The terms related to ρ_{23}, however, are unique to the collision of orthogonal simultons in a three-level system and any difference we find in the collision of solitary waves in a three-level system compared to the collision of solitary waves in two-level systems should thus be attributed to those terms.

In Fig. 6 the influence of the solitary wave collision on the coherences in the system is shown. The rightward-moving pulse is polarized in y direction and the leftward-moving pulse in x direction. In the case of the undisturbed simulton [see Fig. 6(a)] the coherence ρ_{12}, which gives rise to the optical polarization in y direction, is symmetric in time and it helps to preserve the shape of the symmetric pulse. The collision with the counterpropagating pulse changes this picture considerably [see Fig. 6(b)]. At the spatial symmetry point of the collision,

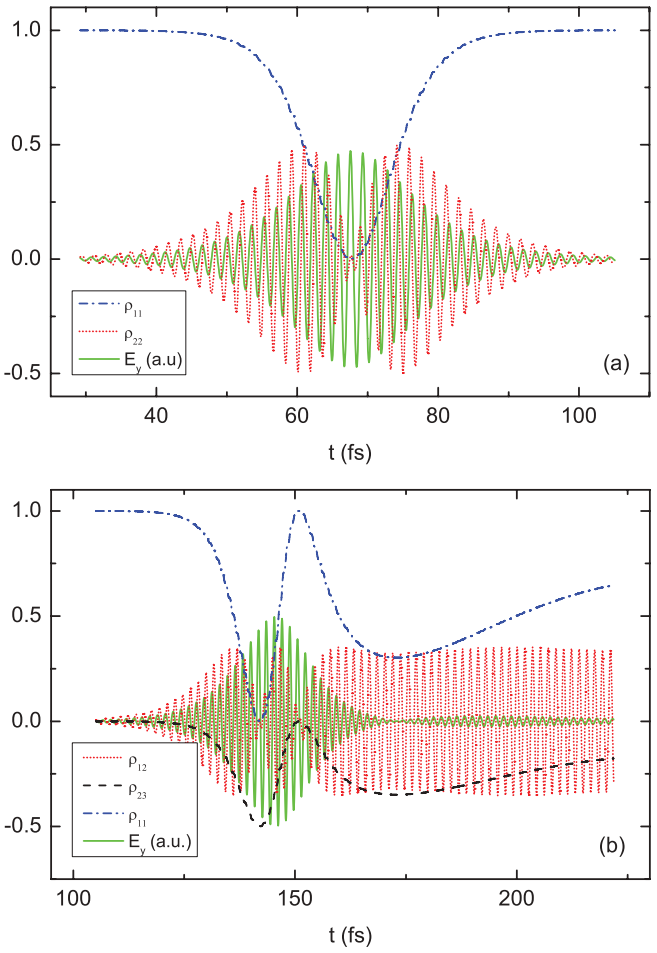

FIG. 6. (Color online) (a) Re (ρ_{12}) (dotted red line), ρ_{11} (dash-dotted blue line), and E_y (solid green line) and of an undisturbed simulton of group velocity $v_0 = 0.75c$ in a three-level system plotted against time in units of the inverse frequency. (b) Re (ρ_{12}) (dotted red line), ρ_{11} (dash-dotted blue line), E_y (solid green line), and Re (ρ_{23}) (black dashed line) at the symmetry point of a collision between two counterpropagating simultons of group velocity $v_0 = 0.75c$, one resonant with the $1 \leftrightarrow 2$ transition (E_y), the other resonant with the $1 \leftrightarrow 3$ transition (E_z).

the leading edge of coherence ρ_{12} behaves similarly to the case of the undisturbed simulton, but ρ_{12} does not rise to $1/2$ anymore. Its trailing edge is first shortened, then rises again, and stays almost on a constant level for a prolonged period of time, thereby producing a second electric field pulse. The magnitude of the real part of the coherence ρ_{23} reaches a maximum value of $1/2$ and influences the coherence ρ_{12} as shown in Eq. (15). This influence together with the influence of the counterpropagating pulse on the occupation probabilities of the levels reshapes the optical polarization and destroys its symmetry, leading to the breakup of the pulse and the birth of a new soliton.

All above investigations can only be of practical relevance if they still hold true when a small dephasing rate is added to the equations. Our numerical experiments confirm that the collisions are not significantly affected by small dephasing rates. Small dephasing rates do, however, cause a selective excitation of a small region inside the medium under certain

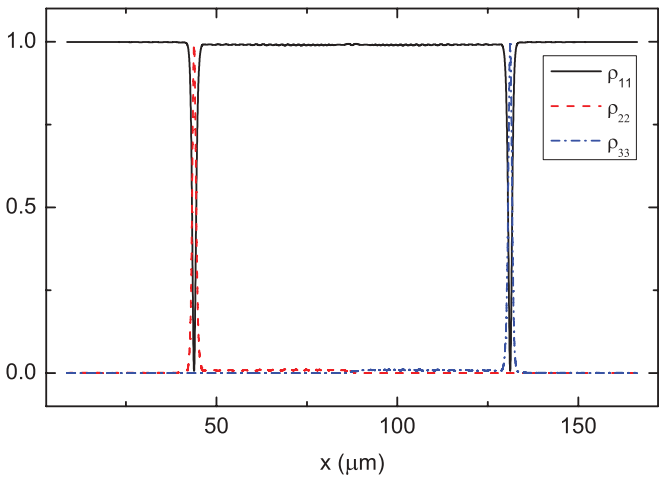

FIG. 7. (Color online) Occupancies of a three-level medium with dephasing long after the collision of two simultons with orthogonal polarization. Parameters used were $\lambda = 525\,\text{nm}$, $\mu = 2.8 \times 10^{-29}\,\text{C m}$, $n = 1.87 \times 10^{24}\,\text{m}^{-3}$, $\tau = 2.66 \times 10^{-15}\,\text{s}$ (four-cycle pulse), and $\gamma_{12} = \gamma_{13} = 57\,\text{ns}^{-1}$, resulting in a primary pulse velocity of $v_0 = 0.863c$.

conditions. If we add dephasing to the system, fast pulses with a group velocity on the order of the speed of light will not be affected much. They still propagate almost lossless through the medium, whereas the slow pulses created in the collision may be completely absorbed inside the system, if they are slow enough compared to the dephasing time. This makes it possible to invert the population in a small region close to the collision region of the pulses without exciting the rest of the medium. Figure 7 illustrates this possibility. Such a selective excitation has in the past been reported to be achievable in three-level Λ-media [25,34], but to the best of our knowledge no scheme has been proposed to do so in a V-type medium.

C. Collision of simultons with arbitrary polarizations

The collision of simultons with the same field polarization is very different from the collision of simultons with orthogonal field polarizations. This observation leads us to expect some kind of intermediate behavior between a two-level case and a genuine three-level case for simultons with some arbitrary angle between the two field polarizations. In this section we investigate this intermediate behavior by switching gradually between a two-level and a three-level case. To this end, we take the three-level medium as outlined in Sec. II and study how counterpropagating linearly polarized simultons collide. One of the solitons is E_z polarized, whereas the other is polarized with an angle α relative to the z axis.

The subject of investigation is the dependence of the group velocity of the faster simulton (or only simulton if there is no soliton birth) resulting from the collision on the angle of relative polarization α (see Fig. 8). For low polarization angles α the collision is very similar to the collision in the two-level case. The group velocities v_1 do not change much for low angles, whereas the variation in group velocity is relatively steep when we approach orthogonal polarization. Qualitatively, the collision outcome is also much closer to the two-level case for most polarization angles. For a group

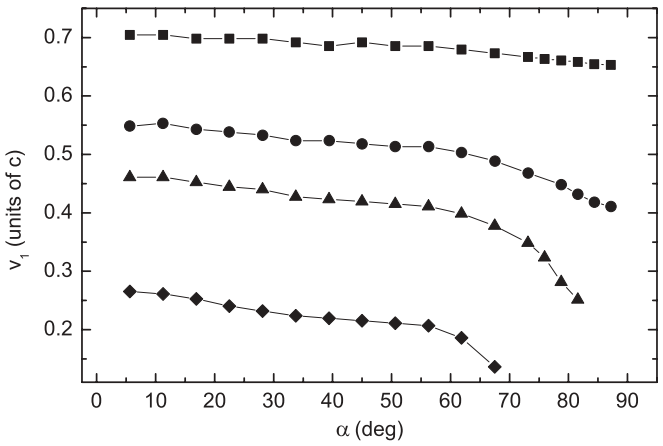

FIG. 8. Group velocity v_1 after collision plotted over angle α between polarizations of counterpropagating simultons for initial group velocities of $v_0 = 0.75c$ (squares), $v_0 = 0.65c$ (circles), $v_0 = 0.6c$ (triangles), and $v_0 = 0.5c$ (diamonds).

velocity of $v_0 = 0.5c$ no simulton would be expected after collision in the three-level case but it would be expected for the two-level case. Up to an angle of about 70° the initial simulton is attenuated but still present after the collision. The genuine three-level case of pulse breakup is only observed for higher angles. For an initial group velocity of $v_0 = 0.75c$, a soliton birth can only be observed if the polarization angle is above 80°.

These results paint a relatively clear picture of the nature of the interaction process. The collision behavior resembles the collision behavior of orthogonal polarizations only for angles close to 90°. This indicates that, if a substantial fraction of the pulses are parallel polarized, the interaction mediated by the population density dominates over the interaction mediated by the coherence.

IV. CONCLUSION

We analyzed the collision process of two counterpropagating simultons of pulse area 2π using a three-level medium in a one-dimensional finite-difference time-domain model. The implementation avoids the usual rotating wave, slowly varying envelope and unidirectional propagation approximations and allows us to accurately simulate the collision of simultons.

The birth of additional simultons can occur in a degenerate three-level medium, if the individual pulses are resonant (or near resonant) with the transitions and have (close-to) orthogonal relative polarizations. Additional solitary waves are found if the group velocities of the original pulses are higher than a critical group velocity of $v_0 \approx 0.62c$ and the difference in group velocities between the resulting pulses gets larger with higher initial group velocities. Below this critical group velocity the original pulses break up into two or more co-moving, inseparable solutions. As a change in the angle between the polarizations of the interacting pulses results in a different collision outcome, such collisions provide a possible mechanism to enact polarization and amplitude-dependent interaction schemes between light pulses.

In a dissipative three-level medium, counterpropagating simultons of group velocity close to the speed of light could be used to excite a population inversion in a small region next to the collision region of the pulses as the resulting very slow simultons will be absorbed in a dissipative medium whereas the fast original pulses will propagate almost unaffected. In contrast, two pulses with a group velocity slightly higher than the critical velocity could be used to create additional pulses.

Since the crucial parameters in the system such as density of the active medium, pulse length, pulse amplitude, and light polarization can be controlled experimentally it should be possible to observe the effects described in this paper in an experiment using, for example, gas-filled hollow core fibers [35].

ACKNOWLEDGMENTS

We gratefully acknowledge support from the Engineering and Physical Sciences Research Council.

APPENDIX: NUMERICAL MODEL

The propagation of the light pulses is modeled on the basis of the one-dimensional finite-difference time-domain method [26]:

$$\mathbf{H}\left(t+\frac{\Delta t}{2},x+\frac{\Delta x}{2}\right)=\mathbf{H}\left(t+\frac{\Delta t}{2},x+\frac{\Delta x}{2}\right)+\frac{\Delta t}{\Delta x}[\mathbf{E}(t,x+\Delta x)-\mathbf{E}(t,x)] \tag{A1}$$

$$\mathbf{D}(t+\Delta t,x)=\mathbf{D}(t,x)+\frac{\Delta t}{\Delta x}\left[\mathbf{H}\left(t+\frac{\Delta t}{2},x+\frac{\Delta x}{2}\right)-\mathbf{H}\left(t+\frac{\Delta t}{2},x-\frac{\Delta x}{2}\right)\right], \tag{A2}$$

$$\mathbf{E}(t+\Delta t,x)=\frac{1}{\epsilon(x)}[\mathbf{D}(t+\Delta t,x)-\mathbf{P}(t+\Delta t,x)], \tag{A3}$$

combined with Mur boundary conditions [27].

The local electric field, which couples to the three-level Bloch equations of the material, is calculated from the electric displacement **D** as

$$\mathbf{E}_{\rm loc}(t,x)=\frac{1}{\epsilon}\left[\mathbf{D}(t,x)-\frac{2}{3}\mathbf{P}(t,x)\right], \tag{A4}$$

with

$$\mathbf{P}(t,x)=n\,\mathrm{tr}\,[\hat{\rho}(t,x)\hat{\boldsymbol{\mu}}]=2n\sum_{i\neq j}\mathrm{Re}\,[\boldsymbol{\mu}_{ij}^{*}\rho_{ij}(t,x)]. \tag{A5}$$

We integrate the material Bloch equations at every grid cell by a fourth-order Runge-Kutta scheme, where we interpolate the electric displacement **D** to get the values of the electric field at the halfway points. A similar scheme has been applied successfully by Loiko and Serrat in [25]. The scheme has been tested for its numerical stability and accuracy, and it behaves perfectly well for any realistic Rabi frequencies.

[1] J. S. Russell, Report on Waves, *Report of the Fourteenth Meeting of the British Association for the Advancement of Science, York, September 1844* (London, 1845), pp. 311–390, Plates XLVII-LVII.
[2] N. N. Akhmediev, Opt. Quantum Electron. **30**, 535 (1998).
[3] D. D. Yavuz, D. R. Walker, and M. Y. Shverdin, Phys. Rev. A **67**, 041803(R) (2003).
[4] G. Assanto and G. Stegeman, Opt. Express **10**, 388 (2002).
[5] M. Segev, B. Crosignani, A. Yariv, and B. Fischer, Phys. Rev. Lett. **68**, 923 (1992).
[6] S. L. McCall and E. L. Hahn, Phys. Rev. Lett. **18**, 908 (1967).
[7] A. A. Afanas'ev, V. M. Volkov, V. V. Dritz, and B. A. Samson, J. Mod. Opt. **37**, 165 (1990).
[8] M. J. Shaw and B. W. Shore, J. Opt. Soc. Am. B **8**, 1127 (1991).
[9] N. N. Rosanov, V. E. Semenov, and N. V. Vyssotina, Laser Phys. **17**, 1311 (2007).
[10] B. A. Malomed and S. Wabnitz, Opt. Lett. **16**, 1388 (1991).
[11] A. Peleg, M. Chertkov, and I. Gabitov, J. Opt. Soc. Am. B **21**, 18 (2004).
[12] G. I. Stegeman and M. Segev, Science **286**, 1518 (1999).
[13] O. Cohen, R. Uzdin, T. Carmon, J. W. Fleischer, M. Segev, and S. Odoulov, Phys. Rev. Lett. **89**, 133901 (2002).
[14] M. S. Petrovic, M. R. Belic, C. Denz, and Y. S. Kivshar, Laser Photonics Rev. (2010).
[15] W. Krolikowski, B. Luther-Davies, C. Denz, and T. Tschudi, Opt. Lett. **23**, 97 (1998).
[16] W. Krolikowski and S. A. Holmstrom, Opt. Lett. **22**, 369 (1997).
[17] J. Andrade Lucio, B. Alvarado Mendez, R. Rojas-Laguna, O. Ibarra-Manzano, M. Torres-Cisneros, R. Jaime-Rivas, and E. Kuzin, Electron. Lett. **36**, 1403 (2000).
[18] M. Erkintalo, G. Genty, and J. M. Dudley, Opt. Express **18**, 13379 (2010).
[19] S. L. McCall and E. L. Hahn, Phys. Rev. **183**, 457 (1969).
[20] J. C. Eilbeck, J. D. Gibbon, P. J. Caudrey, and R. K. Bullough, J. Phys. A **6**, 1337 (1973).
[21] H. Steudel and A. A. Zabolotskii, J. Phys. A: Math. Gen. **37**, 5047 (2004).
[22] A. I. Maimistov, A. M. Basharov, S. O. Elyutin, and Y. M. Sklyarov, Phys. Rep. **191**, 1 (1990).
[23] Q.-Han Park and H. J. Shin, Phys. Rev. A **57**, 4643 (1998).
[24] A. Rahman, Phys. Rev. A **60**, 4187 (1999).
[25] Y. Loiko and C. Serrat, Phys. Rev. A **73**, 063809 (2006).
[26] K. Yee, IEEE Trans. Antennas Propag. **14**, 302 (1966).
[27] G. Mur, IEEE T. Electromagn. C. **23**, 377 (1981).
[28] C. M. Bowden and J. P. Dowling, Phys. Rev. A **47**, 1247 (1993).
[29] K. Xia, S. Gong, C. Liu, X. Song, and Y. Niu, Opt. Express **13**, 5913 (2005).
[30] A. Taflove and S. C. Hagness, *Computational Electrodynamics: The Finite-Difference Time-Domain Method*, 3rd Ed. (Artech House, Norwood, 2005).
[31] A. V. Tarasishin, S. A. Magnitskii, V. A. Shuvaev, and A. M. Zheltikov, Opt. Express **8**, 452 (2001).
[32] H. Steudel, J. Mod. Opt. **35**, 693 (1988).
[33] S. V. Branis, O. Martin, and J. L. Birman, Phys. Rev. A **43**, 1549 (1991).
[34] Y. Loiko, C. Serrat, R. Vilaseca, V. Ahufinger, J. Mompart, and R. Corbalan, Phys. Rev. A **75**, 023801 (2007).
[35] A. V. Gorbach and D. V. Skryabin, Opt. Express **16**, 4858 (2008).